

# Charm-Quark Contribution to $K_L \rightarrow \mu^+ \mu^-$ at Next-to-Next-to-Leading Order

Martin Gorbahn<sup>1</sup> and Ulrich Haisch<sup>2</sup>

<sup>1</sup>*Institut für Theoretische Teilchenphysik, Universität Karlsruhe, D-76128 Karlsruhe, Germany*

<sup>2</sup>*Institut für Theoretische Physik, Universität Zürich, CH-8057 Zürich, Switzerland*

(Dated: September 25, 2006)

We calculate the charm-quark contribution to the decay  $K_L \rightarrow \mu^+ \mu^-$  in next-to-next-to-leading order of QCD. This new contribution reduces the theoretical uncertainty in the relevant parameter  $P_c$  from  $\pm 22\%$  down to  $\pm 7\%$ , corresponding to scale uncertainties of  $\pm 3\%$  and  $\pm 6\%$  in the short-distance part of the branching ratio and the determination of the Wolfenstein parameter  $\bar{\rho}$  from  $K_L \rightarrow \mu^+ \mu^-$ . The error in  $P_c = 0.115 \pm 0.018$  is now in equal shares due to the combined scale uncertainties and the current uncertainty in the charm-quark mass. We find  $\mathcal{B}(K_L \rightarrow \mu^+ \mu^-)_{\text{SD}} = (0.79 \pm 0.12) \times 10^{-9}$ , with the present uncertainty in the Cabibbo-Kobayashi-Maskawa matrix element  $V_{td}$  being the dominant individual source in the quoted error.

PACS numbers: 12.15.Hh, 12.38.Bx, 13.20.Eb

The study of the rare process  $K_L \rightarrow \mu^+ \mu^-$  has played a central role in unraveling the flavor content and structure of the standard model (SM) of electroweak interactions [1]. These glory days have passed, but still today  $K_L \rightarrow \mu^+ \mu^-$  provides useful information on the short-distance dynamics of  $|\Delta S| = 1$  flavor-changing-neutral-current transitions despite the fact that its decay amplitude is dominated by the long-distance two photon contribution  $K_L \rightarrow \gamma^* \gamma^* \rightarrow \mu^+ \mu^-$ . While the absorptive part of the latter correction is calculable with high precision in terms of the  $K_L \rightarrow \gamma \gamma$  rate the corresponding dispersive part represents a significant source of theoretical uncertainty. In fact long- and short-distance dispersive pieces cancel against each other in large parts and the

measured total  $K_L \rightarrow \mu^+ \mu^-$  rate [2] is nearly saturated by the absorptive two photon contribution. The precision in the determination of the dispersive pieces therefore controls the accuracy of possible bounds on the real part of the Cabibbo-Kobayashi-Maskawa (CKM) element  $V_{td}$  or, equivalently, the Wolfenstein parameter  $\bar{\rho}$ . In view of the recent experimental [3] and theoretical [4] developments concerning the dispersive long-distance part of the  $K_L \rightarrow \mu^+ \mu^-$  decay amplitude it is also worthwhile to improve the theoretical accuracy of the associated short-distance contribution. This is the purpose of this Letter.

The branching ratio for the dispersive short-distance part of  $K_L \rightarrow \mu^+ \mu^-$  can be written as [5]

$$\mathcal{B}(K_L \rightarrow \mu^+ \mu^-)_{\text{SD}} = \kappa_\mu \left[ \frac{\text{Re}\lambda_t}{\lambda^5} Y(x_t) + \frac{\text{Re}\lambda_c}{\lambda} P_c \right]^2, \quad (1)$$

$$\kappa_\mu \equiv \frac{\alpha^2 \mathcal{B}(K^+ \rightarrow \mu^+ \nu_\mu)}{\pi^2 \sin^4 \theta_w} \frac{\tau(K_L)}{\tau(K^+)} \lambda^8 = (2.009 \pm 0.017) \times 10^{-9} \left( \frac{\lambda}{0.225} \right)^8, \quad (2)$$

where  $\lambda_i \equiv V_{is}^* V_{id}$  denote the relevant CKM factors. There is also a short-distance two-loop electroweak contribution in the two-photon mediated decay amplitude [6]. Following [4], where this contribution is included in the two-photon correction itself, we do not add it to the short-distance contribution in Eq. (1). The apparent strong dependence of  $\mathcal{B}(K_L \rightarrow \mu^+ \mu^-)_{\text{SD}}$  on  $\lambda \equiv |V_{us}|$  is spurious as  $P_c$  is proportional to  $1/\lambda^4$ . In quoting the value for  $P_c$  we will set  $\lambda = 0.225$ . The electromagnetic coupling  $\alpha$  and the weak mixing angle  $\sin^2 \theta_w$  entering  $\mathcal{B}(K_L \rightarrow \mu^+ \mu^-)$  are naturally evaluated at the electroweak scale [7]. Then the leading term in the heavy top expansion of the electroweak two-loop corrections to  $Y(x_t)$  amounts to typically  $-1.5\%$  for the modified mini-

mal subtraction scheme ( $\overline{\text{MS}}$ ) definition of  $\alpha$  and  $\sin^2 \theta_w$  [8]. In obtaining the numerical value of Eq. (2) we have employed  $\alpha \equiv \alpha_{\overline{\text{MS}}}(M_Z) = 1/127.9$ ,  $\sin^2 \theta_w \equiv \sin^2 \hat{\theta}_w^{\overline{\text{MS}}} = 0.231$ , and  $\mathcal{B}(K^+ \rightarrow \mu^+ \nu_\mu) = (63.39 \pm 0.18) \times 10^{-2}$  [9].

The function  $Y(x_t)$  in Eq. (1) depends on the top quark  $\overline{\text{MS}}$  mass through  $x_t \equiv m_t^2(\mu_t)/M_w^2$ . It originates from  $Z$ -penguin and electroweak box diagrams with an internal top quark. As the relevant operator has a vanishing anomalous dimension and the energy scales involved are of the order of the electroweak scale or higher, the function  $Y(x_t)$  can be calculated within ordinary perturbation theory. It is known through next-to-leading order (NLO) [10, 11], with a scale uncertainty due to the top quark matching scale  $\mu_t = \mathcal{O}(m_t)$  of slightly

TABLE I: Input parameters used in the numerical analysis of  $P_c$ ,  $\mathcal{B}(K_L \rightarrow \mu^+ \mu^-)_{\text{SD}}$ , and  $\bar{\rho}$ .

Parameter	Value $\pm$ Error	Reference
$m_c(m_c)$ [GeV]	$1.30 \pm 0.05$	[14], our average
$\alpha_s(M_Z)$	$0.1187 \pm 0.0020$	[9]
$\text{Re}\lambda_t$ [ $10^{-4}$ ]	$-3.11^{+0.13}_{-0.14}$	[15]
$\text{Re}\lambda_c$	$-0.22098^{+0.00095}_{-0.00091}$	[15]

more than  $\pm 2\%$ . Converting the top quark pole mass of  $M_t = (172.5 \pm 2.3)$  GeV [12] at three loops to  $m_t(M_t)$  [13] and relating  $m_t(M_t)$  to  $m_t(m_t) = (162.8 \pm 2.2)$  GeV using the one-loop renormalization group (RG), we find  $Y(x_t) = 0.950 \pm 0.049$ . The given uncertainty combines linearly an error of  $\pm 0.029$  due to the error of  $m_t(m_t)$  and an error of  $\pm 0.020$  obtained by varying  $\mu_t$  in the range  $60 \text{ GeV} \leq \mu_t \leq 240 \text{ GeV}$ .

The calculable parameter  $P_c$  entering Eq. (1) results from  $Z$ -penguin and electroweak box diagrams involving internal charm-quark exchange. As now both high- and low-energy scales, namely,  $\mu_w = \mathcal{O}(M_W)$  and  $\mu_c = \mathcal{O}(m_c)$ , are involved, a complete RG analysis of this term is required. In this manner, large logarithms  $\ln(\mu_w^2/\mu_c^2)$  are resummed to all orders in  $\alpha_s$ . The large scale uncertainty due to  $\mu_c$  of  $\pm 44\%$  in the leading order result was a strong motivation for the NLO analysis of this contribution [5, 11].

Performing the RG running from  $\mu_w$  down to  $\mu_b = \mathcal{O}(m_b)$  in an effective five-flavor theory and the subsequent evolution from  $\mu_b$  down to  $\mu_c$  in an effective four-flavor theory, we obtain at NLO

$$\begin{aligned}
 P_c &= 0.106 \pm 0.023_{\text{theor}} \pm 0.009_{m_c} \pm 0.001_{\alpha_s} \\
 &= (0.106 \pm 0.034) \left( \frac{0.225}{\lambda} \right)^4, \quad (3)
 \end{aligned}$$

where the parametric errors correspond to the ranges of the charm-quark  $\overline{\text{MS}}$  mass  $m_c(m_c)$  and the strong coupling constant  $\alpha_s(M_Z)$  given in Table I. The final error has been obtained by performing a detailed analysis of the individual sources of uncertainty entering the NLO prediction of  $P_c$  using a modified version of the CKMFITTER package [15]. The same statistical treatment of errors will be applied in Eqs. (4), (8), and (9).

The dependence of  $P_c$  on  $\mu_c$  can be seen in Fig. 1. The solid line in the upper plot shows the NLO result obtained by evaluating  $\alpha_s(\mu_c)$  from  $\alpha_s(M_Z)$  solving the RG equation of  $\alpha_s$  numerically, while the dashed and dotted lines are obtained by first determining the scale parameter  $\Lambda_{\overline{\text{MS}}}$  from  $\alpha_s(M_Z)$ , either using the explicit solution of the RG equation of  $\alpha_s$  or by solving the RG equation of  $\alpha_s$  iteratively for  $\Lambda_{\overline{\text{MS}}}$ , and subsequently calculating  $\alpha_s(\mu_c)$  from  $\Lambda_{\overline{\text{MS}}}$ . The corresponding two-loop values for  $\alpha_s(\mu_c)$  have been obtained with the program

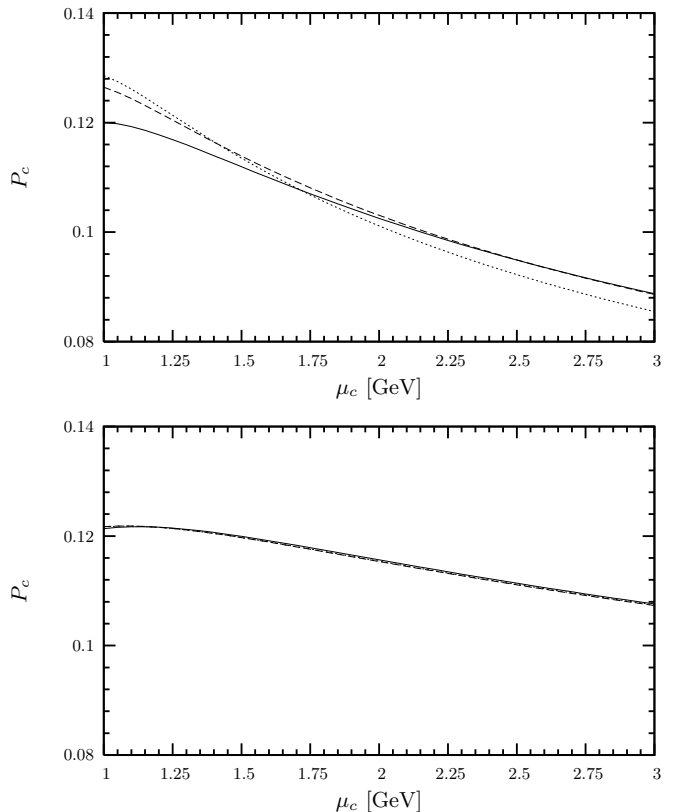


FIG. 1:  $P_c$  as a function of  $\mu_c$  at NLO (upper plot) and NNLO (lower plot). The three different lines correspond to three different methods of computing  $\alpha_s(\mu_c)$  from  $\alpha_s(M_Z)$  (see text).

RUNDEC [16]. Obviously, the difference between the three curves is due to higher order terms and has to be regarded as part of the theoretical error. With its size of  $\pm 0.006$  it is almost comparable to the variation of the NLO result due to  $\mu_c$ , amounting to  $\pm 0.016$ . In [5] a larger value for the latter uncertainty has been quoted. The observed difference is related to the definition of the charm-quark mass. Replacing  $m_c(m_c)$  in the logarithms  $\ln(\mu_c^2/m_c^2)$  of the one-loop matrix elements by the more appropriate  $m_c(\mu_c)$  leads to a significant reduction of the dependence of  $P_c$  on  $\mu_c$ . A detailed discussion of this issue can be found in [17]. Finally, while in [5] only  $\mu_c$  was varied, the theoretical error given in Eq. (3) includes also the dependence on  $\mu_b$  and  $\mu_w$  of combined  $\pm 0.001$ . The specified scale uncertainties correspond to the ranges  $1 \text{ GeV} \leq \mu_c \leq 3 \text{ GeV}$ ,  $2.5 \text{ GeV} \leq \mu_b \leq 10 \text{ GeV}$ , and  $40 \text{ GeV} \leq \mu_w \leq 160 \text{ GeV}$ .

Using the input parameters listed in Table I, we find from Eqs. (1)–(3) at NLO

$$\begin{aligned}
 \mathcal{B}(K_L \rightarrow \mu^+ \mu^-)_{\text{SD}} &= (0.77 \pm 0.08_{P_c} \pm 0.08_{\text{other}}) \times 10^{-9} \\
 &= (0.77 \pm 0.16) \times 10^{-9}, \quad (4)
 \end{aligned}$$

where the second error in the first line collects the uncertainties due to  $\kappa_\mu$ ,  $Y(x_t)$ , and the CKM elements.

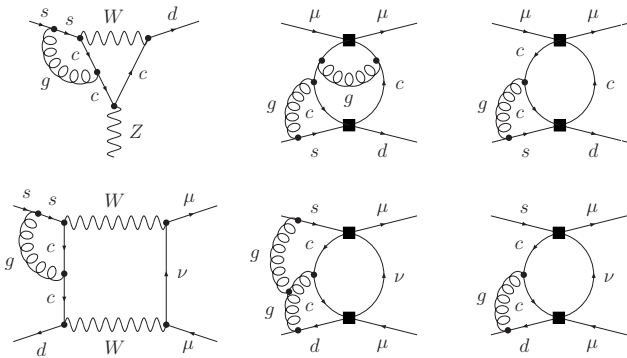


FIG. 2: Examples of Feynman diagrams arising in the full SM (left column), describing the mixing of operators (center column) and the matrix elements (right column) in the  $Z$ -penguin (upper row) and the electroweak box (lower row) sector. Only the divergent pieces of the diagrams displayed in the center column have to be computed, while the Feynman graphs shown on the left- and right-hand side are needed including their finite parts.

As the uncertainties in Eqs. (3) and (4) coming from  $M_t$ ,  $m_c(m_c)$  and the CKM parameters should be decreased in the coming years it is also desirable to reduce the theoretical uncertainty in  $P_c$ . To this end, we here extend the NLO analysis of  $P_c$  presented in [5, 11] to the next-to-next-to-leading order (NNLO). This requires the computation of three-loop anomalous dimensions of certain operators and of certain two-loop contributions.

The main components of the NNLO calculation, which aims at resumming all  $\mathcal{O}(\alpha_s^n \ln^{n-1}(\mu_w^2/\mu_c^2))$  logarithms in  $P_c$ , are (i) the  $\mathcal{O}(\alpha_s^2)$  matching corrections to the relevant Wilson coefficients arising at  $\mu_w$ , (ii) the  $\mathcal{O}(\alpha_s^3)$  anomalous dimensions describing the mixing of the dimension-six and -eight operators, (iii) the  $\mathcal{O}(\alpha_s^2)$  threshold corrections to the Wilson coefficients originating at  $\mu_b$ , and (iv) the  $\mathcal{O}(\alpha_s^2)$  matrix elements of some of the operators emerging at  $\mu_c$ . To determine the contributions of type (i), (iii), and (iv) one must calculate two-loop Green functions in the full SM and in effective theories with five or four flavors. Sample diagrams for steps (i) and (iv) are shown in the left and right columns of Fig. 2. The contributions (ii) are found by calculating three-loop Green functions with operator insertions. Sample diagrams with a double insertion of dimension-six operators are shown in the center column of Fig. 2.

The  $Z$ -penguin contribution can be trivially obtained from that in  $K^+ \rightarrow \pi^+ \nu \bar{\nu}$ , which has been recently computed at NNLO [17, 18]. The electroweak box contribution on the other hand is slightly different for  $K_L \rightarrow \mu^+ \mu^-$  and  $K^+ \rightarrow \pi^+ \nu \bar{\nu}$  since the lepton line in the corresponding Feynman diagrams is reversed and thus requires a new calculation. A comprehensive discussion of the technical details of the matching and the renormalization of the effective theory can be found in [17].

TABLE II: The coefficients  $\kappa_{ijkl}$  arising in the approximate formula for  $P_c$  at NNLO.

$\kappa_{1000} = -0.5373$	$\kappa_{0100} = -6.0472$	$\kappa_{0010} = -0.0956$
$\kappa_{0001} = 0.0114$	$\kappa_{1100} = 3.9957$	$\kappa_{1010} = 0.3604$
$\kappa_{0110} = 0.0516$	$\kappa_{0101} = -0.0658$	$\kappa_{2000} = -0.1767$
$\kappa_{0200} = 16.4465$	$\kappa_{0020} = -0.1294$	$\kappa_{0030} = 0.0725$

In the following we present only the final result for the  $\mathcal{O}(\alpha_s^2)$  matching correction  $C_\mu^{B(2)}$ , the  $\mathcal{O}(\alpha_s^3)$  anomalous dimension  $\gamma_\mu^{B(2)}$ , and the  $\mathcal{O}(\alpha_s^2)$  matrix element  $r_\mu^{B(2)}$ . Employing the operator basis of [5, 11] we obtain for the standard choices of Casimir operators  $C_A = 3$ ,  $C_F = 4/3$ , and  $f$  active quark flavors

$$\begin{aligned}
 C_\mu^{B(2)} &= \frac{416}{3} + \frac{16\pi^2}{3} + \frac{272}{3} \ln \frac{\mu_w^2}{M_W^2} + 16 \ln^2 \frac{\mu_w^2}{M_W^2}, \\
 \gamma_\mu^{B(2)} &= \frac{27032}{9} - 1088 \zeta(3) - \frac{1040}{9} f, \\
 r_\mu^{B(2)} &= -\frac{112}{3} - \frac{80}{3} \ln \frac{\mu_c^2}{m_c^2} - 16 \ln^2 \frac{\mu_c^2}{m_c^2}.
 \end{aligned} \tag{5}$$

Here  $\zeta(x)$  is the Riemann zeta function with the value  $\zeta(3) \approx 1.20206$  and  $m_c \equiv m_c(\mu_c)$  denotes the charm-quark  $\overline{\text{MS}}$  mass. Our results for the NLO Wilson coefficient, the anomalous dimension and the matrix element agree with the findings of [11] where an error made in the original calculation [5] has been corrected.

The analytic expression for  $P_c$  including the complete NNLO corrections is too complicated and too long to be presented here. Instead setting  $\lambda = 0.225$ ,  $m_t(m_t) = 162.8 \text{ GeV}$  and  $\mu_w = 80.0 \text{ GeV}$  we derive an approximate formula for  $P_c$  that summarizes the dominant parametric and theoretical uncertainties due to  $m_c(m_c)$ ,  $\alpha_s(M_Z)$ ,  $\mu_c$ , and  $\mu_b$ . It reads

$$\begin{aligned}
 P_c &= 0.1198 \left( \frac{m_c(m_c)}{1.30 \text{ GeV}} \right)^{2.3595} \left( \frac{\alpha_s(M_Z)}{0.1187} \right)^{6.6055} \\
 &\times \left( 1 + \sum_{i,j,k,l} \kappa_{ijkl} L_{m_c}^i L_{\alpha_s}^j L_{\mu_c}^k L_{\mu_b}^l \right),
 \end{aligned} \tag{6}$$

where

$$\begin{aligned}
 L_{m_c} &= \ln \left( \frac{m_c(m_c)}{1.30 \text{ GeV}} \right), & L_{\alpha_s} &= \ln \left( \frac{\alpha_s(M_Z)}{0.1187} \right), \\
 L_{\mu_c} &= \ln \left( \frac{\mu_c}{1.5 \text{ GeV}} \right), & L_{\mu_b} &= \ln \left( \frac{\mu_b}{5.0 \text{ GeV}} \right),
 \end{aligned} \tag{7}$$

and the sum includes the expansion coefficients  $\kappa_{ijkl}$  given in Table II. The above formula approximates the exact NNLO result with an accuracy of better than  $\pm 1.0\%$  in the ranges  $1.15 \text{ GeV} \leq m_c(m_c) \leq 1.45 \text{ GeV}$ ,  $0.1150 \leq \alpha_s(M_Z) \leq 0.1230$ ,  $1.0 \text{ GeV} \leq \mu_c \leq 3.0 \text{ GeV}$

and  $2.5 \text{ GeV} \leq \mu_b \leq 10.0 \text{ GeV}$ . The uncertainties due to  $m_t(m_t)$ ,  $\mu_w$  and the different methods of computing  $\alpha_s(\mu_c)$  from  $\alpha_s(M_Z)$ , which are not quantified above, are all below  $\pm 0.2\%$ . Their actual size at NNLO will be discussed below.

Using the input parameters listed in Table I, we find at the NNLO level

$$\begin{aligned} P_c &= 0.115 \pm 0.008_{\text{theor}} \pm 0.008_{m_c} \pm 0.001_{\alpha_s} \\ &= (0.115 \pm 0.018) \left( \frac{0.225}{\lambda} \right)^4, \end{aligned} \quad (8)$$

where now the residual scale ambiguities and the uncertainty due to  $m_c(m_c)$  are of the same size. Comparing these numbers with Eq. (3) we observe that our NNLO calculation reduces the theoretical uncertainty by a factor of more than 3.

As can be nicely seen in the lower plot of Fig. 1,  $P_c$  depends very weakly on  $\mu_c$  at NNLO, varying by only  $\pm 0.007$ . Furthermore, the three different treatments of  $\alpha_s$  affect the NNLO result in a negligible way. The three-loop values of  $\alpha_s(\mu_c)$  used in the numerical analysis have been obtained with the program RUNDEC. The theoretical error quoted in Eq. (8) includes also the dependence on  $\mu_b$  and  $\mu_w$  of combined  $\pm 0.001$ . The presented scale uncertainties correspond to the ranges given earlier.

Using Eqs. (1), (2), and (8) the result in Eq. (4) is modified to the NNLO value

$$\begin{aligned} \mathcal{B}(K_L \rightarrow \mu^+ \mu^-)_{\text{SD}} &= (0.79 \pm 0.04_{P_c} \pm 0.08_{\text{other}}) \times 10^{-9} \\ &= (0.79 \pm 0.12) \times 10^{-9}. \end{aligned} \quad (9)$$

Obviously, at present the errors from  $M_t$ ,  $m_c(m_c)$  and the CKM parameters veil the benefit of the NNLO calculation of  $P_c$  presented in this Letter.

Provided both  $P_c$  and  $\mathcal{B}(K_L \rightarrow \mu^+ \mu^-)_{\text{SD}}$  are known with sufficient precision useful bounds on the Wolfenstein parameter  $\bar{\rho}$  can be obtained [5]. In particular for the measured branching ratio  $\mathcal{B}(K_L \rightarrow \mu^+ \mu^-)_{\text{SD}}$  close to its SM predictions, one finds that given uncertainties  $\sigma(P_c)$  and  $\sigma(\mathcal{B}(K_L \rightarrow \mu^+ \mu^-)_{\text{SD}})$  translate into

$$\frac{\sigma(\bar{\rho})}{\bar{\rho}} = \pm 0.89 \frac{\sigma(P_c)}{P_c} \pm 2.59 \frac{\sigma(\mathcal{B}(K_L \rightarrow \mu^+ \mu^-)_{\text{SD}})}{\mathcal{B}(K_L \rightarrow \mu^+ \mu^-)_{\text{SD}}}. \quad (10)$$

As seen in Eq. (10) the accuracy of the determination of  $\bar{\rho}$  depends sensitively on the error in  $P_c$ . The reduction of the theoretical error in  $P_c$  from  $\pm 22\%$  down to  $\pm 7\%$  translates into the following uncertainties

$$\frac{\sigma(\bar{\rho})}{\bar{\rho}} = \begin{cases} \pm 20\%, & \text{NLO,} \\ \pm 6\%, & \text{NNLO,} \end{cases} \quad (11)$$

implying a significant improvement of the NNLO over the NLO result. In obtaining these numbers we have included only the theoretical errors quoted in Eqs. (3) and (8).

Using the conservative upper bound

$$\mathcal{B}(K_L \rightarrow \mu^+ \mu^-)_{\text{SD}} < 2.5 \times 10^{-9}, \quad (12)$$

on the short-distance part of the  $K_L \rightarrow \mu^+ \mu^-$  branching ratio derived in [4], we find the following allowed range

$$-0.74 < \bar{\rho} < 3.13, \quad (13)$$

for the Wolfenstein parameter  $\bar{\rho}$  employing a customized version of the CKMFITTER code.

To conclude, we have evaluated the complete NNLO correction of the charm-quark contribution to  $\mathcal{B}(K_L \rightarrow \mu^+ \mu^-)_{\text{SD}}$ . The inclusion of these contributions leads to a drastic reduction of the theoretical uncertainty in the relevant parameter  $P_c$ . This strengthens the power of the rare decay  $K_L \rightarrow \mu^+ \mu^-$  in determining the Wolfenstein parameter  $\bar{\rho}$  from its short-distance branching ratio.

We would like to thank A. J. Buras and U. Nierste for carefully reading the manuscript, and A. Höcker and J. Ocariz for useful correspondence concerning the CKMFITTER package, and I. Picek and S. Trine for informative communications regarding the two-loop electroweak two-photon contribution. U. H. has been supported by the Schweizer Nationalfonds.

**Note added:** There is an additional contribution from anomalous triangle diagrams to  $P_c$  not included in our work. The numerical effect of this mistake is negligible, see the erratum of [17] for details.

- 
- [1] S. L. Glashow, J. Iliopoulos and L. Maiani, Phys. Rev. D **2**, 1285 (1970); M. K. Gaillard and B. W. Lee, Phys. Rev. D **10**, 897 (1974).
  - [2] D. Ambrose *et al.* [E871 Collaboration], Phys. Rev. Lett. **84**, 1389 (2000).
  - [3] A. Alavi-Harati *et al.* [KTeV Collaboration], Phys. Rev. Lett. **87**, 071801 (2001); **90**, 141801 (2003).
  - [4] G. Isidori and R. Unterdorfer, JHEP **0401**, 009 (2004) and references therein.
  - [5] G. Buchalla and A. J. Buras, Nucl. Phys. B **412**, 106 (1994).
  - [6] J. O. Eeg, K. Kumericki and I. Picek, Eur. Phys. J. C **1**, 531 (1998).
  - [7] C. Bobeth *et al.*, JHEP **0404**, 071 (2004).
  - [8] G. Buchalla and A. J. Buras, Phys. Rev. D **57**, 216 (1998).
  - [9] S. Eidelman *et al.* [Particle Data Group], Phys. Lett. B **592** (2004) 1, and 2005 partial update for edition 2006 available at <http://pdg.lbl.gov/>.
  - [10] G. Buchalla and A. J. Buras, Nucl. Phys. B **398**, 285 (1993); B **400**, 225 (1993); M. Misiak and J. Urban, Phys. Lett. B **451**, 161 (1999).
  - [11] G. Buchalla and A. J. Buras, Nucl. Phys. B **548**, 309 (1999).
  - [12] E. Brubaker *et al.* [The Tevatron Electroweak Working Group], hep-ex/0603039.

- [13] K. G. Chetyrkin and M. Steinhauser, Phys. Rev. Lett. **83**, 4001 (1999); Nucl. Phys. B **573**, 617 (2000); K. Melnikov and T. v. Ritbergen, Phys. Lett. B **482**, 99 (2000).
- [14] J. H. Kühn and M. Steinhauser, Nucl. Phys. B **619**, 588 (2001) [Erratum-ibid. B **640**, 415 (2002)]; J. Rolf and S. Sint [ALPHA Collaboration], JHEP **12**, 007 (2002); A. H. Hoang and M. Jamin, Phys. Lett. B **594**, 127 (2004); O. Buchmüller and H. Flächer, Phys. Rev. D **73**, 073008 (2006); A. H. Hoang and A. V. Manohar, Phys. Lett. B **633**, 526 (2006); K. G. Chetyrkin, J. H. Kühn and C. Sturm, hep-ph/0604234; R. Boughezal, M. Czakon and T. Schutzmeier, hep-ph/0605023.
- [15] J. Charles *et al.* [CKMfitter Group], Eur. Phys. J. C **41**, 1 (2005), and updated results available at <http://ckmfitter.in2p3.fr>.
- [16] K. G. Chetyrkin, J. H. Kühn and M. Steinhauser, Comput. Phys. Commun. **133**, 43 (2000).
- [17] A. J. Buras *et al.*, JHEP **0611**, 002 (2006) [hep-ph/0603079v3].
- [18] A. J. Buras *et al.*, Phys. Rev. Lett. **95**, 261805 (2005).